

# LIMITS AND POSSIBILITIES OF LASER PLASMA ACCELERATORS: DEMONSTRATION OF STAGING TWO INDEPENDENTLY POWERED MODULES\*

S. Steinke, J. van Tilborg, C. Benedetti, C. G. R. Geddes, C. B. Schroeder, J. Daniels<sup>1,2</sup>,  
K. K Swanson<sup>1</sup>, A. J. Gonsalves, K. Nakamura, B. H. Shaw<sup>1</sup>, E. Esarey, W. P. Leemans<sup>†</sup>  
Lawrence Berkeley National Laboratory, Berkeley, CA 94720, U. S. A.

<sup>1</sup>also at University of California - Berkeley, Berkeley, CA 94720, U. S. A.

<sup>2</sup>also at Eindhoven University of Technology, 5600MB Eindhoven, The Netherlands

## Abstract

We present experimental results where two laser-plasma-accelerator (LPA) [1] stages are coupled at a short distance by a plasma mirror. Stable electron beams from the first stage were used to longitudinally probe the dark-current-free, quasi-linear wakefield excited by the laser of the second stage. Changing the arrival time of the electron beam with respect to the second stage laser pulse allowed reconstruction of the temporal wakefield structure, determination of the plasma density, and inference of the length of the electron beam. The first stage electron beam could be focused by an active plasma lens [2] to a spot-size smaller than the transverse wake size at the entrance of the second stage. This permitted electron beam trapping, verified by an 100 MeV energy gain [3].

## INTRODUCTION

A broad range of future science applications, from particle colliders beyond 1 TeV [4] to compact free-electron lasers and Thomson  $\gamma$ -ray sources, motivates advanced acceleration techniques such as LPA to overcome the limitations of conventional accelerator technology [5]. Within the last several years tremendous progress in LPA development has been made. After the first demonstration of percent level energy spread and small divergence in mm-scale plasmas in 2004 [6–8], GeV electron beams were obtained with 40 TW laser pulses, and subsequently electron beams with multi-GeV energies [9] were reported with PW-class laser systems and few-cm plasmas [10–12]. Controlling the injection of electrons into plasma waves enabled precise tunability of the accelerator [13–15].

For staging of two LPAs, the required component techniques have been developed and are each operating reliably, and experiments to combine these components were performed and staging was successfully demonstrated [3]. The components are a stable first LPA, plasma lens

for transport/focusing of the first stage electron beam, plasma mirror coupling of the second stage laser to preserve high gradient, and a second stage with accelerating field, as well as supporting experimental systems. A schematic is shown in Fig. 1.

## INJECTOR STAGE

For this reason, a first stage using a gas jet plasma has been implemented. Several gas jets with different profiles were tested and characterized. A mixture of two gases (99% helium and 1% nitrogen) was used to increase the amount of trapped charge. In such a mixed gas, injection was achieved by ionizing deeply bound electron from a high atomic number gas (nitrogen) near the peak of the laser pulse, the proper phase inside the wakefield allowing them to be trapped. Scalable, stable beams in the range 70 MeV to 120 MeV with 60% energy spread, beam charge of 30 pC, and low divergence ( $4\pm 0.3$ ) mrad were routinely produced with a pointing stability of 0.3 mrad (standard deviation) over hours of run time, corresponding to thousands of laser shots and more than 10 days (see Fig. 2).

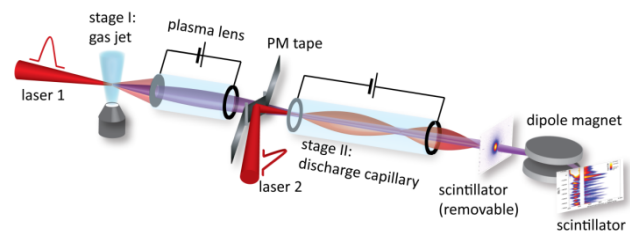


Figure 1: Staging experimental schematic, showing the first stage LPA (stage I), plasma lens, plasma mirror (PM), which couples the laser pulse for the second stage LPA, second stage LPA (stage II) and electron beam diagnostics (dipole magnet and scintillator) [3].

These beams provide the stability required for staging. Remaining jitter is highly correlated to the performance of the (15 year old) front-end laser system. To ensure coupling of significant charge to the second stage wake, the first stage must have low electron beam divergence and low pointing jitter.

\* This work was supported by the U.S. Department of Energy Office of Science Office of High Energy Physics, under Contract No. DE-AC02-05CH11231, by the U.S. Department of Energy National Nuclear Security Administration, Defense Nuclear Nonproliferation R&D (NA22) and by the National Science Foundation (NSF) under contracts 0917687 and 0935197. This research used computational resources (Edison, Hopper) of the National Energy Research Scientific Computing center (NERSC), which is supported by the Office of Science of the U.S. Department of Energy under Contract No. DE-AC02-05CH11231.

† Email address: wpleemans@lbl.gov

### ACTIVE PLASMA LENS

The electron beams generated in the first stage were transported to the second stage target using a pulsed active plasma lens [2]. Radially-symmetric focusing was achieved in a gas-filled 15 mm long capillary with a

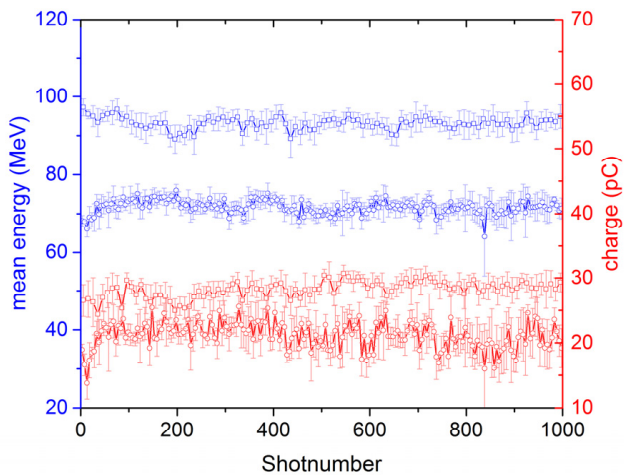


Figure 2: Stable operation of the first stage of the staging experiment (using a mixture of 99% He and 1% N<sub>2</sub>). Mean energy (blue) and charge (red) versus shot number of 1000 consecutive shots. The two data sets (squares and circles) represent two regimes in which stable electron beams could be generated.

diameter of 500  $\mu\text{m}$  using an axial discharge current of 650 A, which produced an azimuthal focusing magnetic field. The high field strengths produced ( $\sim 0.5$  T) re-focused electrons of energy range 75–125 MeV in a distance of 25 mm through the plasma mirror (PM) tape to an energy-dependent spot size of  $\sigma = 20\text{--}30$   $\mu\text{m}$  (rms) at the second plasma stage. Divergence acceptance of the lens was 5 mrad. We performed an experimental characterization of the use of a discharge-capillary active plasma lens to transport 100-MeV-level electron beams produced by a laser-plasma accelerator. The plasma lenses can have field gradients in excess of 3000 T/m, allowing for the focusing of GeV-level electron beams over distances of a few cm. By changing the magnetic field strength, we showed focusing with weak chromatic dependencies and (after an extra oscillation at higher currents) with stronger chromatic dependencies. By incorporating the spatial and energy resolution of the magnetic spectrometer, excellent agreement of the data to simulation was retrieved (see Fig. 3). The electron beam size at the optimum focused energy was 0.81 mm (rms). This is consistent with an upper-bound LPA geometrical emittance of  $\lesssim 7$  nm (source size  $\lesssim 5$   $\mu\text{m}$ ) talking into account emittance growth in the PM tape.

### PLASMA MIRROR

Coupling of the two stages at a short distance is important both to efficiently couple the first stage beam into the second stage, and to preserve high geometric gradient. To achieve this, the PM developed in past years has been improved and systems have been implemented to allow its operation without disruption in between the stages.

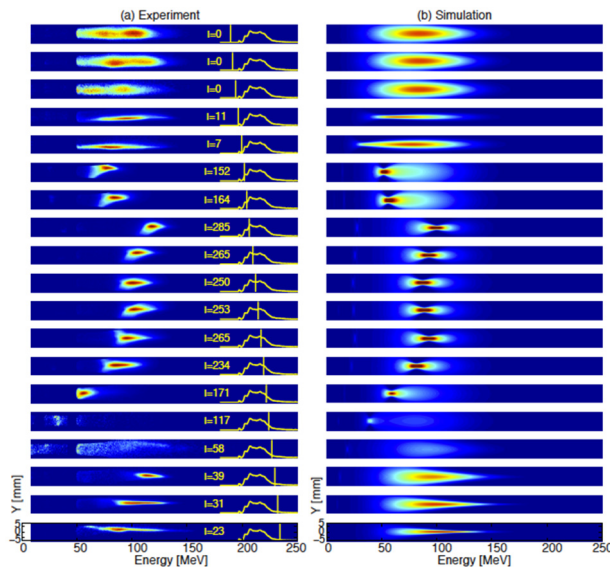


Figure 3: Effects of capillary lensing on the electron beam energy spectra as a function of discharge current (left). The observed data is in good agreement with simulations of electron beam transport using a TWISS model for the capillary lens (right) [2].

The PM is a solid density plasma which, being over-dense, reflects the driver laser pulse of the second stage LPA, but which must be thin such that the first stage electron beam passes through it. This is achieved using a tape drive to present a new, micron thick surface to reflect the laser on each shot. The tape drive tension, velocity, and tape supports have been precisely made and refined to reduce pointing jitter of the reflected laser (see Fig. 4a). Jitter of the laser mode centroid in the focal plasma of the laser comparable to that of the input laser has been achieved, as required for coupling to the second stage capillary. Quality of the reflected laser is also sufficient, with 80% reflection and with high mode quality at focusing (Strehl ratio of 0.8) suitable for coupling distances of  $\sim 5$  mm from the tape to the second stage. This PM study was done for the magnetic and plastic (non-magnetic) sides of the VHS tape, and for input light of both s- and p-polarization (see Fig. 4b).

The laser pulse fluence was varied by changing the focal position relative to the tape surface, which changed the spot size at the tape.

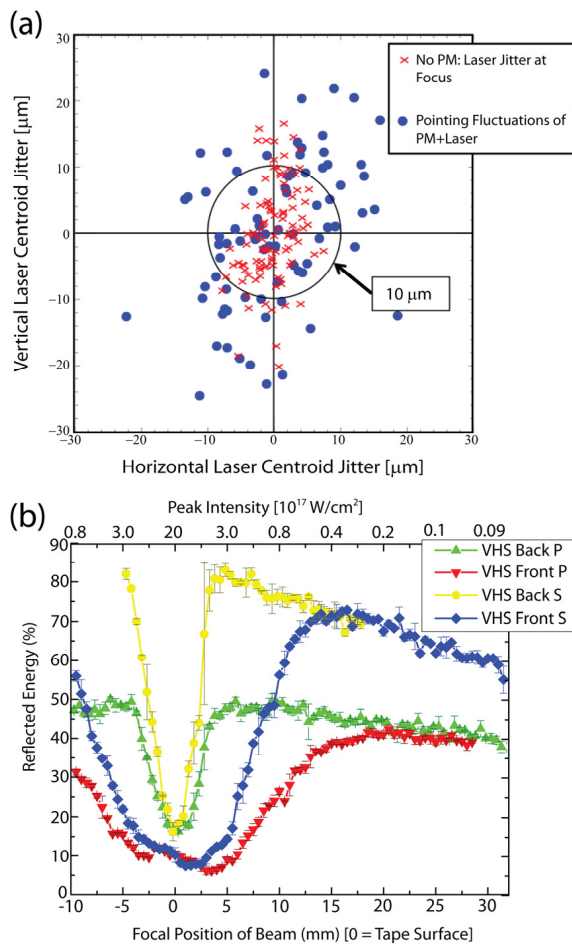


Figure 4: (a) Input laser jitter at focus (red x) and PM pointing fluctuations (blue circles) were measured as the standard deviation of the laser spot's centroid to the beam axis. (b) Plot showing the reflected energy from both the plastic and iron oxide sides of a VHS tape plasma mirror using s and p-polarized light. The focal position of the laser pulse was scanned longitudinally in order to scan the input intensity of the laser pulse at the tape surface.

## COUPLING OF TWO INDEPENDENT LPA STAGES

The laser pulses reflected off the PM were guided in the parabolic plasma channel created in the discharge capillary with an energy transmission of 85%. Wake excitation under these conditions was confirmed by measuring optical spectra of the transmitted laser pulse, showing an increasing redshift with increasing plasma density in the channel. Quantitative analysis of the spectra revealed a maximum relative redshift of 3% with respect to the central wavelength of the laser at a density of  $2 \times 10^{18} \text{ cm}^{-3}$ . This corresponds to an average field amplitude of  $\sim 17 \text{ MV/mm}$  if wake excitation occurs over the full length of the capillary.

To control the phasing of the electron beam in the plasma wake of the second stage LPA, the delay between the two laser pulses driving the first and the second stages

was varied with fs precision by an optical delay stage in the laser beam line of the injector stage. Electron spectra were recorded as a function of the delay between the two laser pulses. In the case of a positive delay, the first stage electrons propagated without the influence of the second laser pulse. After the second laser pulse arrived (negative delay), the electron spectra were periodically modulated in energy (Fig. 5a). The period of the modulation was  $(80 \pm 6) \text{ fs}$ , consistent with a plasma wavelength  $\lambda_p = 24 \mu\text{m}$  at a density of  $(1.9 \pm 0.3) \times 10^{18} \text{ cm}^{-3}$ . The constant periodicity of the observed modulation as a function of delay behind the driver pulse further indicates a quasi-linear wake, consistent with expectations for the experimental parameters including laser intensity and plasma density.

The resulting electron distributions are plotted in Fig. 5b in the form of a waterfall plot of electron spectra where each horizontal line corresponds to a 5-shot averaged energy spectrum. Background-subtracted 2D charge maps, also averaged over 5 shots, are shown in Fig. 5d-g for significant delays. The presence of the second-stage laser results in a reduction of total beam charge of up to a factor of 3 (see Fig. 5a). For appropriate timing of the second stage laser, however, charge was detected beyond the energy cut-off of the input electron spectrum, i.e.,  $>200 \text{ MeV}$ . This charge accelerated beyond the cut-off of the input spectrum, shown by the red and yellow areas in Figs. 5d, and 5f, indicates acceleration in the second stage. The integrated charge in this region of  $1.2 \text{ pC}$  represents the charge trapped in the accelerating phase of the wake and a trapping efficiency of 3.5%. At delays of  $\lambda_p/2$  after the times of maximum energy gain,  $\sim 1 \text{ pC}$  of additional charge was detected around 110–150 MeV (Figs. 5e and 5g). This could correspond to electrons decelerated or to electrons deflected by the transverse wake fields into the spectrometer acceptance. The broad energy spread of the first stage electron beam prevents unambiguous observation of the decelerating phase of the wake under these conditions.

Numerical modelling performed allows detailed analysis of the interaction. Figure 6a shows reference-subtracted electron spectra as a function of the delay between the arrival of the electron bunch and the laser pulse.

The simulations show that the observed energy modulations depend on the phasing of the electron bunch within the wake. The periodicity of the modulation is determined by the plasma density and is consistent with the experimental observation. However, the amount of post accelerated charge decreases in the later accelerating phases of the wake as a result of increasing wake curvature. The fact that the linearity of the wake appears to be preserved in the experimental results could be attributed to a deviation from the (transverse) parabolic plasma density profile. It was shown that, e.g., simulating a quartic plasma density profile yields a charge distribution similar to that obtained in the experiment (see Fig. 6b).



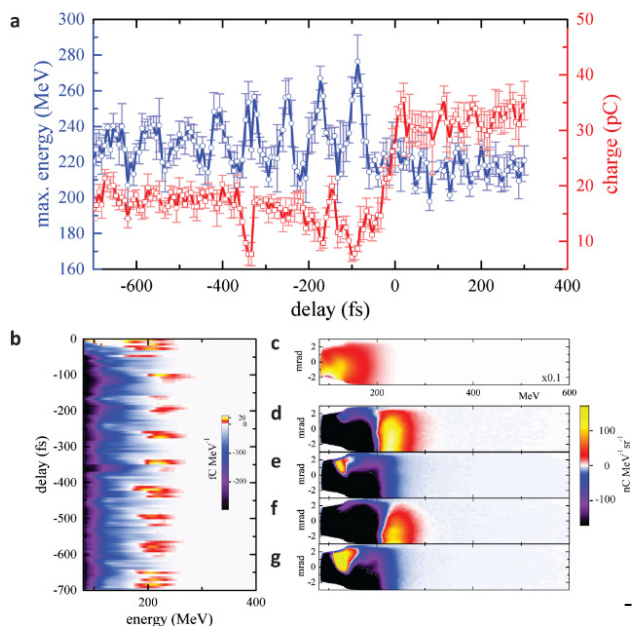


Figure 5: Spectra of electron beams from staged acceleration: (a) Maximum electron energy (blue) and total electron beam charge (red) as a function of the delay of the two driving laser pulses. A single data point represents an average of 5 measurements and the error bar the standard deviation. (b) Waterfall plot of electron spectra (5-shot average), each with the reference subtracted, as function of delay. (c) 100-shot average unperturbed reference for delays of 100-300 fs before arrival of the second laser pulse. (d)–(g) 2D charge maps (5-shot average) subtracted by the reference (c) for the first two maxima and minima of the energy oscillation shown in (a), i.e. for delays of -107 fs, -153 fs, -193 fs, and -240 fs, respectively [3].

### CONCLUSIONS

In summary, we have presented an experimental study of staging of two LPAs independently driven by two synchronized laser pulses. Electron beam injection and capture into the second stage wake was demonstrated by means of an  $\sim 100$  MeV energy gain recurring at delays corresponding to multiples of  $\lambda_p$ . The observation of temporally well-defined energy modulations further directly implies a bunch length of the input electron beam shorter than  $\lambda_p/4 \sim 5 \mu\text{m}$ . This represents a major milestone in the development of laser driven plasma-based accelerators towards future colliders, as well as any other LPA application that requires electron energies beyond the single-stage limits.

### ACKNOWLEDGEMENT

The authors thank N. H. Matlis, S. Shiraiishi, and T. Sokollik for their contributions to the initial construction of the setup and an early version of the experiment, as well as C. Toth, D. Syversrud, N. Ybarrolaza, M. Kirkpatrick G. Mannino, T. Sipla, D. Evans, R. Duarte, D. Baum and D. Munson for their contributions.

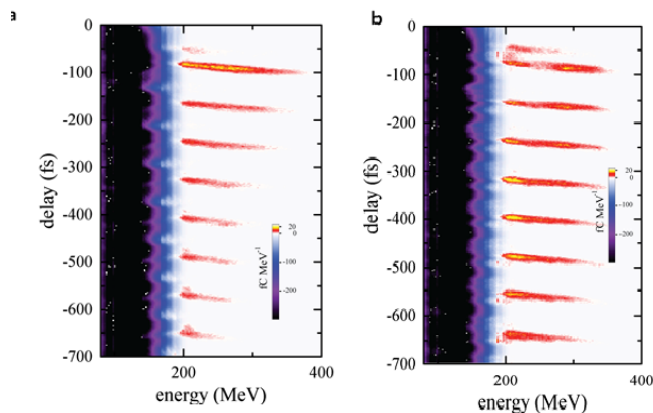


Figure 6: Simulation results: Waterfall plot of electron spectra as function of delay for plasma channels with transversely parabolic- (a) and quartic- (b) plasma density profiles. Each spectrum was subtracted by the reference in a similar way as for the experimental result in Fig. 5b [3].

### REFERENCES

- [1] E. Esarey, C. B. Schroeder, and W. P. Leemans, *Reviews of Modern Physics* **81**, 1229 (2009).
- [2] J. van Tilborg *et al.*, *Physical Review Letters* **115**, 184802 (2015).
- [3] S. Steinke *et al.*, *Nature* **530**, 190 (2016).
- [4] J. Ellis and I. Wilson, *Nature* **409**, 431 (2001).
- [5] C. B. Schroeder, E. Esarey, C. G. R. Geddes, C. Benedetti, and W. P. Leemans, *Phys Rev Spec Top-Ac* **13**, 101301, 101301 (2010).
- [6] C. G. R. Geddes, C. Toth, J. van Tilborg, E. Esarey, C. B. Schroeder, D. Bruhwiler, C. Nieter, J. Cary, and W. P. Leemans, *Nature* **431**, 538 (2004).
- [7] S. P. D. Mangles *et al.*, *Nature* **431**, 535 (2004).
- [8] J. Faure, Y. Glinec, A. Pukhov, S. Kiselev, S. Gordienko, E. Lefebvre, J. P. Rousseau, F. Burgy, and V. Malka, *Nature* **431**, 541 (2004).
- [9] W. P. Leemans, B. Nagler, A. J. Gonsalves, C. Toth, K. Nakamura, C. G. R. Geddes, E. Esarey, C. B. Schroeder, and S. M. Hooker, *Nature Physics* **2**, 696 (2006).
- [10] W. P. Leemans *et al.*, *Physical Review Letters* **113**, 245002 (2014).
- [11] X. M. Wang *et al.*, *Nature Communications* **4**, 1988 (2013).
- [12] H. T. Kim, K. H. Pae, H. J. Cha, I. J. Kim, T. J. Yu, J. H. Sung, S. K. Lee, T. M. Jeong, and J. Lee, *Physical Review Letters* **111**, 165002 (2013).
- [13] A. J. Gonsalves *et al.*, *Nature Physics* **7**, 862 (2011).
- [14] J. Faure, C. Rechatin, A. Norlin, A. Lifschitz, Y. Glinec, and V. Malka, *Nature* **444**, 737 (2006).
- [15] F. Amiranoff *et al.*, *Physical Review Letters* **81**, 995 (1998).